

# EMC3 Is Essential for Retinal Organization and Neurogenesis During Mouse Retinal Development

Xiaowen Cao,<sup>1,2</sup> Jianhong An,<sup>1,2</sup> Yuqing Cao,<sup>1,2</sup> Juan Lv,<sup>1,2</sup> Jiawei Wang,<sup>1,2</sup> Yang Ding,<sup>1,2</sup> Xinhua Lin,<sup>3</sup> and Xiangtian Zhou<sup>1,2</sup>

<sup>1</sup>School of Optometry and Ophthalmology and Eye Hospital, Wenzhou Medical University, Wenzhou, Zhejiang, China

<sup>2</sup>State Key Laboratory of Optometry, Ophthalmology and Vision Science, Wenzhou, Zhejiang, China

<sup>3</sup>State Key Laboratory of Genetic Engineering, School of Life Sciences, Zhongshan Hospital, Fudan University, Shanghai, China

Correspondence: Xinhua Lin, State Key Laboratory of Genetic Engineering, School of Life Sciences, Zhongshan Hospital, Fudan University, 2005 Songhu Road, Shanghai 200438, China; [mlin@fudan.edu.cn](mailto:mlin@fudan.edu.cn).

Xiangtian Zhou, State Key Laboratory of Genetic Engineering, School of Life Sciences, Zhongshan Hospital, Fudan University, 2005 Songhu Road, Shanghai 200438, China; [xzt@mail.eye.ac.cn](mailto:xzt@mail.eye.ac.cn).

XC and JA contributed equally to this work.

**Received:** September 22, 2020

**Accepted:** January 18, 2021

**Published:** February 19, 2021

Citation: Cao X, An J, Cao Y, et al. EMC3 is essential for retinal organization and neurogenesis during mouse retinal development. *Invest Ophthalmol Vis Sci.* 2021;62(2):31. <https://doi.org/10.1167/iovs.62.2.31>

**PURPOSE.** We used a mouse model to explore the role of the endoplasmic reticulum membrane protein complex subunit 3 (EMC3) in mammalian retinal development.

**METHODS.** The transcription pattern of *Emc3* in C57BL/6 mice was analyzed by in situ hybridization. To explore the effects of EMC3 absence on retinal development, the Cre-loxP system was used to generate retina-specific *Emc3* in knockout mice (*Emc3*<sup>lox/lox</sup>, *Six3-cre*<sup>+</sup>; CKO). Morphological changes in the retina of E13.5, E17.5, P0.5, and P7 mice were observed via hematoxylin and eosin staining. Immunofluorescence staining was used to assess protein distribution and terminal deoxynucleotidyl transferase dUTP nick end labeling (TUNEL) staining to assess apoptosis changes. Proteins were identified and quantified by Western blotting and proteomic analysis. Electroretinogram (ERG), fundus color photography, and optical coherence tomography were performed on 5-week-old mice to evaluate retinal function and structure.

**RESULTS.** The *Emc3* mRNA was widely distributed in the whole retina during development. Loss of retinal EMC3 led to retinal rosette degeneration with mislocalization of cell junction molecules ( $\beta$ -catenin, N-cadherin, and zonula occludens-1) and polarity molecules (Par3 and PKC $\zeta$ ). Endoplasmic reticulum stress and TUNEL apoptosis signals were present in retinal rosette-forming cells. Although the absence of EMC3 promoted the production of photoreceptor cells, 5-week-old mice lost all visual function and had severe retinal morphological degeneration.

**CONCLUSIONS.** EMC3 regulates retinal structure by maintaining the polarity of retinal progenitor cells and regulating retinal cell apoptosis.

**Keywords:** endoplasmic reticulum membrane protein complex subunit 3 (EMC3), retinal development, retinal rosette, mouse

Visual perception is strictly dependent on the coordinated differentiation and correct assembly of multiple cell types in the retinal structure. Regarding the development of the vertebrate neuroretina, six cell types, including five kinds of neuronal cells (photoreceptors, horizontal slender cells, bipolar cells, amacrine cells, and retinal ganglion cells) and one kind of glial cells (Müller cells), are all generated from the retinal progenitor cells (RPCs), resulting in high tissue complexity.<sup>1–4</sup> During cell differentiation, retinal cell morphology and retinal structure are regulated by cell polarity.<sup>5</sup> Cell junction and cell polarity proteins, such as  $\beta$ -catenin,<sup>6</sup> N-cadherin,<sup>7–9</sup> and polarity protein complex Par3 / Par3 / PKC $\zeta$ ,<sup>10,11</sup> have been reported to play crucial roles in the development of retinal structure.

The endoplasmic reticulum membrane protein complex (EMC) is a widely expressed and conserved complex,<sup>12,13</sup> that in mammals is composed of 10 subunits.<sup>14</sup> The EMC plays roles in protein trafficking, endoplasmic reticulum stress (ERS), lipid homeostasis, organelles communication,

autophagy, virus maturation, and lung development,<sup>15–21</sup> among other functions. Recent studies have also shown that the EMC is a transmembrane domain insertion enzyme and mediates insertion of proteins into the lipid bilayer.<sup>22,23</sup> EMC3, a subunit of EMC, plays a unique role in the retina. The *emc3* homologue in zebrafish is required for the survival of red cone photoreceptors,<sup>24,25</sup> and the deletion of EMC3 in *Drosophila* affects the biosynthesis of rhodopsin.<sup>19,26</sup> Knocking out the *Emc3* gene in mouse photoreceptor cells leads to the mislocalization of rhodopsin and the death of photoreceptor cells.<sup>26</sup> However, the role of EMC3 in structural development of the retina and neurogenesis during mammalian ocular development, especially in the early stages, is not clear.

Here, we generated a retina-specific *Emc3* knockout (CKO) mouse line by mating *Six3-Cre* (retina-specific expression of *Cre*) mice<sup>27</sup> with *Emc3*<sup>lox/+</sup> mice.<sup>21</sup> We performed morphological, functional, immunofluorescent, and expression studies of the retina to explore the role of EMC3

at different stages of mouse retinal development. We also performed proteomic studies to identify proteins that may mediate the developmental role of EMC3 in retinal development. The findings we report here provide insights into the role of EMC3 in mammalian retinal development.

## MATERIALS AND METHODS

### Mice

All mice had a C57BL/6 background (GemPharmatech Co. Ltd, Nanjing, China) and were raised in a specific pathogen free environment under a 12 hour / 12 hour light-dark cycle. Retina-specific *Emc3* knockout mice (CKO, *Emc3<sup>fllox/fllox</sup>, Six3-Cre<sup>+</sup>*) were generated by crossing *Emc3<sup>fllox/+</sup>* with *Six3-Cre<sup>+</sup>* mice (#019755; The Jackson Laboratory, Bar Harbor, ME, USA). Control mice (genotypes: *Emc3<sup>fllox/fllox</sup>, Six3-Cre<sup>-</sup>*) were obtained during breeding. *Emc3<sup>fllox/+</sup>* mice were generated from *Emc3<sup>TG/+</sup>* mice<sup>21</sup> (*Emc3<sup>tm1a(EUCOMM)Wtsi</sup>*, MGI #4453751). *Six3-Cre* is expressed throughout the retina from E9, and the expression was highest in the central region.<sup>27</sup> The mice were mated regularly at 5 PM every day, and the appearance of a copulation plug at 8 AM the next day was considered as E0.5. Pregnant mice were euthanized by CO<sub>2</sub> inhalation, and embryos were harvested at E11.5, E13.5, E15.5, and E17.5 for subsequent experiments. For follow-up experiments, postnatal mice were euthanized by anesthesia using a mixture of ketamine (96 mg/kg) and xylazine (14.4 mg/kg) via intraperitoneal injection for follow-up experiments. All animal experiments were conducted in accordance with the Association for Research in Vision and Ophthalmology Statement for the Use of Animals in Ophthalmic and Vision Research and were approved by the Animal Care and Ethics Committee at Wenzhou Medical University. All experiments were performed using at least three animals of each genotype per group.

### Morphology and RNAscope In Situ Hybridization

Paraffin-embedded sections were stained with hematoxylin and eosin (H&E) and RNAscope.<sup>28</sup> Briefly, mouse eyes were removed and immersed overnight in fixation solution composed of methanol: chloroform: glacial acetic acid (6: 3: 1). After alcohol dehydration, the eyes were embedded in paraffin. Paraffin slices (5 μm) were prepared and transferred onto a charged slide for use.

In situ hybridizations were performed using an RNAscope kit (RNAscope 2.5 HD Assay-Red, #322360; ACDBio Co., Newark, CA, USA). The experiments were performed according to the manufacturer's instructions. After hybridization and amplification, the samples were counterstained with hematoxylin. Positive and negative controls were simultaneously set for each experiment (Supplementary Fig. S1). All probes (Mm-Emc3, #500121; negative control probe DapB, #310043; and positive control probe Mm-Polr2a, #312479) were from ACDBio Company.

### Electroretinogram Recording

Electroretinograms (ERGs) were measured with a RETI-port ERG system (Ganzfeld Q450 SC; Roland Consult, Bradenburg, Germany). Following dark adaptation for more than 2 hours, the mice were anesthetized, and the eyes dilated. Then, with the mouse on a heating pad at 37°C, gold circle electrodes were placed on both corneas, together with a

drop of 1% methylcellulose. A stainless-steel needle reference electrode was inserted into each cheek, and a stainless-steel needle ground electrode was inserted into the base of the tail. Five gradient flashing light stimuli with stimulation intensities of 0.0002, 0.0063, 0.20, 2, and 6.3 cd/m<sup>2</sup> were used to induce a scotopic response. Subsequently, 25 cd/m<sup>2</sup> of bright light was applied for 10 minutes of bright adaptation, and then 5 gradients of 0.20, 0.63, 2, 6.3, and 20 cd/m<sup>2</sup> were used to induce the photopic response. ERG results were reported at 2 cd/m<sup>2</sup> intensity.

### Color Fundus Photography and Optical Coherence Tomography

The retinal fundus and retinal structure were visualized using the Phoenix Micron IV imaging system (Phoenix, Pleasanton, CA, USA). The mydriatic and anesthetized mice were placed on the bracket, and using ofloxacin ointment as a medium, the optical lens (light source wavelength 830 nm) was moved close to the cornea along the visual axis. The fundus color photographs and optical coherence tomography (OCT) images were collected synchronously in real-time.

### Immunofluorescence and Terminal Deoxynucleotidyl Transferase dUTP Nick end Labeling

For immunofluorescence, the mouse eyes were enucleated and fixed with 4% formaldehyde in phosphate-buffered saline for 30 minutes. After the tissue was dehydrated using a sucrose gradient, it was embedded in an optimal cutting temperature compound and quickly frozen with liquid nitrogen. Sections (10 μm) were incubated with 10% donkey serum for 2 hours for blocking. Then, sections were incubated overnight at 4°C with one of the following antibodies: IRE1 alpha (p Ser724) antibody (rabbit, 1:500; NB100-2323; Novus Biologicals, Centennial, CO, USA); ZO-1 antibody (rabbit, 1:200; ab96587; Abcam, Cambridge, UK); N-cadherin antibody (rabbit, 1:200; ab76057; Abcam); Par3 antibody (rabbit, 1:500; 07-330; Merck-Millipore, Burlington, MA, USA); protein kinase C (PKC) ζ antibody (mouse, 1:20; sc-17781; Santa Cruz Biotechnology, Dallas, TX, USA); recoverin antibody (rabbit, 1:500; ab5585; Abcam); prospero homeobox protein 1 (Prox1) antibody (rabbit, 1:100; ABN278, Sigma-Aldrich, St. Louis, MO, USA); Ki67 antibody (rabbit, 1:500; ab15580, Abcam); or phospho-Histone H3 (Ser10; pH3) antibody (rabbit, 1:100; 06-570; Merck-Millipore). Following incubation with the primary antibody, the sections were incubated with Alexa Fluor secondary antibody for 2 hours. TUNEL was performed using an In Situ Cell Death Detection Kit (12156792910; Roche, Basel, Switzerland) according to the manufacturer's instructions. Finally, the samples were stained with 4',6-diamidino-2-phenylindole (DAPI). The images were obtained with a Zeiss LSM 880 (Zeiss, Oberkochen, Germany) microscope.

### Cell Counts

To quantify cells in different mouse groups, immunolabeled cells in the central retinal sections with the optic nerve were manually counted. The retinas were divided into six equal parts. The average number of cells from six images obtained

from each of the six retinal parts was used as a sample. Three mice were assessed in each group.

### Western Blotting

Retinas were homogenized in radioimmunoprecipitation assay buffer (RIPA) lysis buffer. After ultrasound and adjustment of protein concentrations, equal amounts of protein were loaded into sodium dodecyl sulfate-polyacrylamide gels. Standard Western blotting procedures were performed. EMC3 antibody (mouse, 1:500; HPA042372; Sigma-Aldrich), cyclic AMP-dependent transcription factor ATF-6 alpha (ATF6) antibody (rabbit, 1:500; NBP1-40256; Novus Biologicals), and  $\alpha$ -tubulin antibody (mouse, 1:1000; 660331-1lg; ProteinTech Group, Rosemont, IL, USA) were incubated overnight at 4°C. The samples were then incubated with the IRDye Secondary Antibody (LI-COR; Biosciences, Lincoln, NE, USA), and signals were visualized using a near-infrared imaging system (Odyssey CLX, LI-COR; Biosciences) and quantified using the ImageJ software. The  $\alpha$ -tubulin was used as a loading control. All the original Western blot bands were displayed (Supplementary Fig. S2).

### Proteomics

Control and CKO retinas ( $n = 3$  each group) at E17.5 and P7 were used for tandem mass spectrometry-based label-free proteomics. The raw data were identified and quantified using the MaxQuant software (version number 1.5.3.17). The proteomics data were deposited to the ProteomeXchange Consortium (<http://proteomecentral.proteomexchange.org>) with an ID PXD023349 via the iProX partner repository<sup>29</sup> (<https://www.iprox.org>, IPX0002708000) and are freely available. Data were normalized with the average for three repeat control samples, and the statistically significant changes were determined using the  $t$ -test. Proteins with significant changes (fold change  $>1.2$  or  $<0.8$ ,  $P < 0.05$ ) were analyzed and enriched using ToppGene (<https://toppgene.cchmc.org/>), and GraphPad Prism 8 (GraphPad Software, Inc., San Diego, CA, USA) was used to generate heatmaps.

### Statistics and Reproducibility

All data were expressed as mean  $\pm$  standard error of the mean, and GraphPad Prism 8 (GraphPad Software, Inc.) was used for statistics and graphing. At least three mice were tested in each experiment. Statistical significance was tested using two-tailed Student's  $t$ -test, with pairing values derived from the same experiment. In the results,  $P < 0.05$  indicates a statistically significant difference ( $*P < 0.05$ ;  $**P < 0.01$ ; and  $***P < 0.001$ ).

## RESULTS

### EMC3 is Required for the Mouse Retinal Structure

To identify the patterns of *Emc3* gene expression in the developing retina, we performed RNAscope in situ hybridization to characterize the retinal sections of mice in different developmental stages. We found that the *Emc3* gene was widely expressed throughout the retina from early (E11.5 and E15.5; Figs. 1A, 1A', 1B, 1B') to late (P0.5 and P7) stages (Figs. 1C, 1C', 1D, 1D') of retinal development. Cepko et al. found that RPC is the main cell type in the early

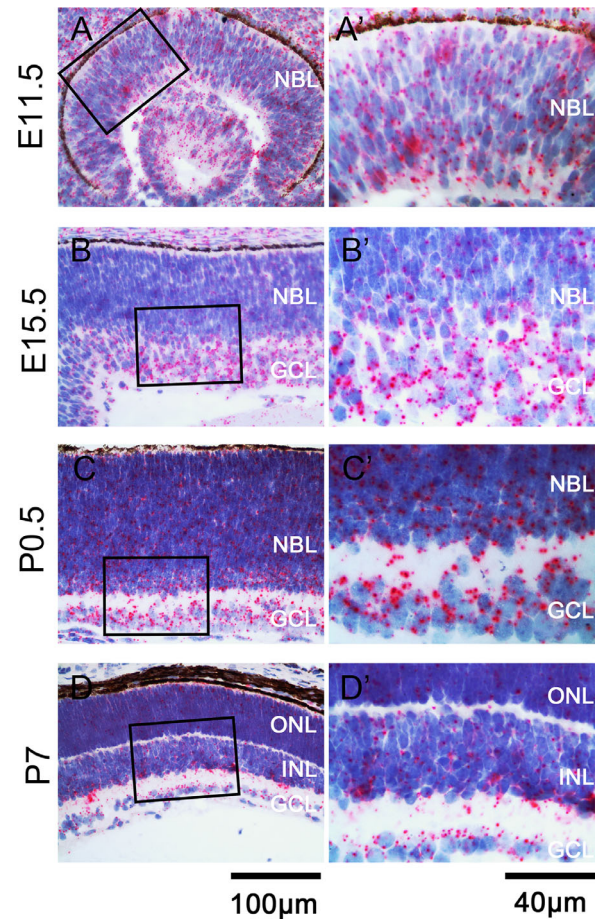


**FIGURE 1.** *Emc3* transcription pattern in C57BL/6 mouse retinas at different stages of development. For E11.5 (A, A'), E15.5 (B, B'), P0.5 (C, C'), and P7 (D, D') C57BL/6 mouse retina, RNAscope indicates that *Emc3* was widely expressed in all layers of the retina. Red dots represent *Emc3* mRNA signal. Left column A–D: 400  $\times$  magnification; right column A'–D': outlined region in left column at 1000  $\times$  magnification. *Emc3*, endoplasmic reticulum membrane protein complex subunit 3; NBL, neuroblastic layer; ONL, outer nuclear layer; INL, inner nuclear layer; GCL, ganglion cell layer.

stages, while differentiated cells are more abundant in the late stages of development.<sup>30</sup> These results indicated that EMC3 was expressed in both RPCs and differentiated cells, suggesting that EMC3 is involved in the regulation of the different stages of retinal development. This was consistent with the results of a previous single-cell sequencing study.<sup>31</sup>

To explore the developmental role of EMC3 in retinal structure and neurogenesis, we generated a retina-specific *Emc3* knockout mouse line (CKO) by crossing mice *Six3-Cre* (for retina-specific expression of *Cre*) with *Emc3<sup>lox/+</sup>* mice (Fig. 2A). The EMC3 level in CKO mice retinas was reduced by about 60% compared to that in control retinas at P7, indicating that EMC3 was successfully deleted (Fig. 2B).

The ERG showed that the electrophysiological signals of CKO mice disappeared both in scotopic and photopic responses (Fig. 2C). With the loss of vision function, further OCT fundus examination showed that the CKO mice retinas were severely thinned, and the fundus blood vessels had almost disappeared (Fig. 2D). To clarify the details of retinal degeneration, we performed H&E staining to analyze retinal morphology. The results showed that the outer nuclear layer,

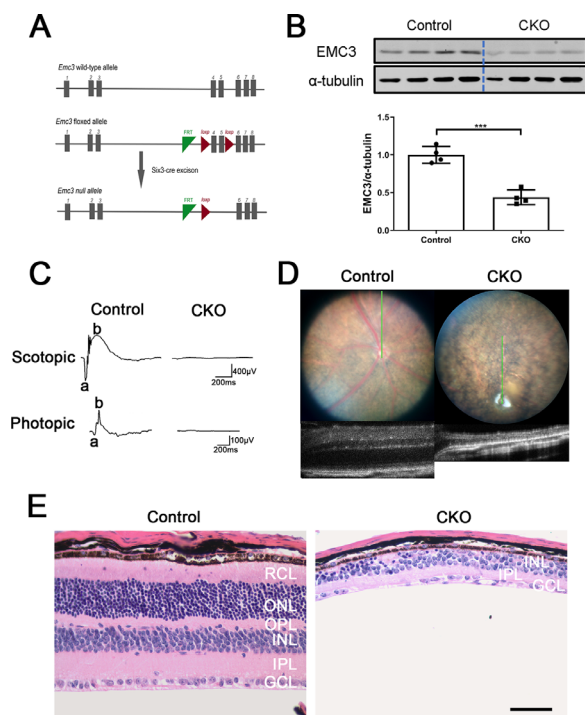


**FIGURE 2. Retina-specific *Emc3* knockout caused disruption of the retinal structure and function.** (A) Strategy for CKO mouse generation. CKO mice were obtained by cross breeding *Emc3<sup>fllox/fllox</sup>* mice and *Six3-cre* mice. (B, upper) Western blot detected the efficiency of the EMC3 knockout in P7 mouse retinas. Grayscale analysis (B, lower) showed that EMC3 was decreased by 56%. The  $\alpha$ -tubulin was the normalized standard. \*\*\* $P < 0.001$ , unpaired, 2-tailed Student's *t*-test. (C) ERG recordings of 5W mice at a stimulus intensity of 2 cd/m<sup>2</sup>. CKO mice had neither a scotopic nor photopic wave, which means that the CKO mice completely lost visual function ( $n = 5$ ). (D) Color fundus photographs and OCT of 5W mice. CKO mouse fundus images had changes in fundus pigments. CKO mouse OCT images revealed severe thinning, and the fundus blood vessels were almost completely absent. (E) H&E staining showed morphological changes in 5W mice. CKO mouse retinas were extremely thin, and the RCL, ONL, and INL had almost disappeared. RCL, rod and cone layer; ONL, outer nuclear layer; OPL, outer plexiform layer; INL, inner nuclear layer; IPL, inner plexiform layer; GCL, ganglion cell layer. Scale bars: 40  $\mu$ m.

inner nuclear layer, and ganglion cell layer had almost disappeared in CKO mice retinas (Fig. 2E). The morphology at the four time points during retinal developmental (E13.5, E17.5, P0.5, and P7) showed the initial effects (Fig. 3). There was no obvious difference between the CKO mice retinas and the control retinas at E13.5 (Figs. 3A, 3A'); however, retinal rosette degeneration, a typical phenotype of retinal structural abnormalities, especially in retinoblastoma,<sup>32–34</sup> and ganglion layer thinning appeared in the central region of the CKO mice retinas at E17.5 (Figs. 3B, 3B'), and retinal degeneration was aggravated as development progressed (Figs. 3C, 3D'). These changes indicated that EMC3 plays a role in the early stages of retinal development.

### Loss of EMC3 in the Retina Caused Mislocalization of Cell Junction and Polarity Proteins

To determine if cell junction and cell polarity participate in rosette formation, we examined the localization of cell junction molecules and cell polarity determinants. In CKO

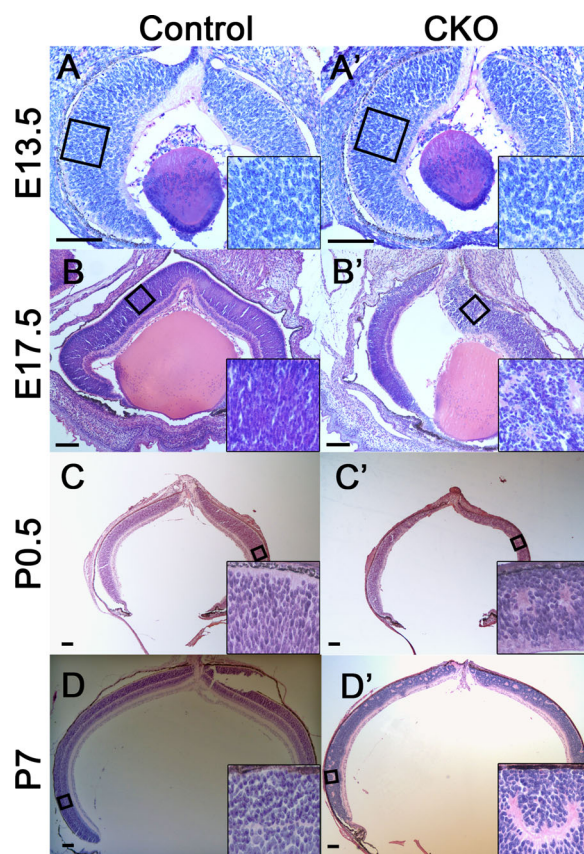


**FIGURE 3. Developing CKO mouse retinas formed rosette structures.** (A–D') H&E staining showed morphological changes in E13.5, E17.5, P0.5, and P7 mice. Retinal rosettes appeared in E17.5, P0.5, and P7 CKO mice. Rosettes first emerged near the optic nerve (B'), and during the developmental process, they spread to through entire retina further into the development process (C', D'). Inset images are magnified picture of the outlined region. Scale bars: 40  $\mu$ m.

mice retinas, the adhesion junction proteins ( $\beta$ -catenin and N-cadherin) and the tight junction protein ZO-1 were mislocalized, especially at P0.5 (Figs. 4A–C; tile scan images in Supplementary Figs. S3–S5). Further, the localizations of cell polarity determinants PKC $\zeta$  and Par3 were similar to one another and dispersed from the apical edge of CKO mice retinas (Fig. 4D). These findings indicated that the loss of EMC3 in the retina led to a change in retinal polarity. However, the expression level of these proteins did not change in P0.5, according to Western blotting results (Figs. 4E–H).

### EMC3 Controls ATPase Activity-Related Proteins

Previous studies have shown that EMC3 was essential for the correct insertion of several transmembrane proteins.<sup>16,19,26</sup> Thus, we analyzed the effects of EMC3 on transmembrane proteins at E17.5 and P7. Proteomic analysis of the CKO mice retinas showed that membrane proteins accounted for 45.82% or 46.73% of the downregulated proteins at E17.5 or P7, respectively (Figs. 5A, 5B). Gene ontology analysis of the downregulated proteins showed that they are involved in ATPase activity, purine ribonucleoside triphosphate binding, and pyrophosphatase activity at E17.5 (Fig. 5C). The downregulated proteins at P7 were related to cation transmembrane transporter activity, transmembrane transporter

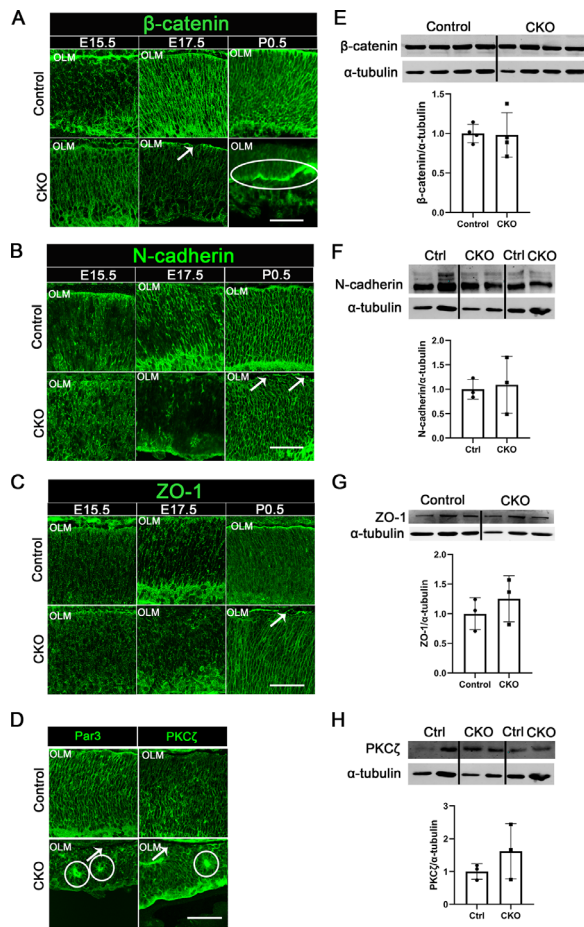


**FIGURE 4. Cell polarity and cell junctions were disrupted in CKO mouse retinas.** (A–C) E15.5, E17.5, and P0.5 retinal sections were immunostained with  $\beta$ -catenin **A**, N-cadherin **B**, and ZO-1 **C** antibodies (green). White arrows indicate the absence of OLM. The white circle represents the dislocated expression on the inner surface of the rosette. OLM, outer limit membrane. Scale bars: 50  $\mu$ m. (D) Immunofluorescence indicated that PAR3 and PKC $\zeta$  gathered on the inner wall of the rosette cavity in P0.5 CKO mice. (E–H) Western blots and quantitation were performed to detect  $\beta$ -catenin **E**, N-cadherin **F**, ZO-1 **G**, and PKC $\zeta$  **H** in P0.5 mice. The  $\alpha$ -tubulin was the normalized standard.

activity, and transporter activity (Fig. 5D). Whether at E17.5 or P7, the significantly downregulated proteins were ATPase activity-related and were responsible for ion transport (Figs. 5E, 5F). These membrane pump proteins exhibit some basic physiological cellular functions including cell adhesion, polarity, and motility.<sup>35–38</sup>

### Loss of EMC3 Caused the Unfolded Protein Response

The unfolded protein response (UPR) occurs when unfolded or misfolded proteins are abundant in the endoplasmic reticulum.<sup>39,40</sup> Three pathways were involved in the UPR, namely inositol-requiring enzyme 1 $\alpha$  (IRE1), activating transcription factor 6 (ATF6), and protein kinase R-like endoplasmic reticulum kinase (PERK). Immunofluorescence analysis showed that the expression of pIRE1 $\alpha$  increased in CKO mice retinas from E15.5 to P0.5 (Fig. 6A). The expression of cleaved ATF6 (50 kDa), and the active form of ATF6 in another

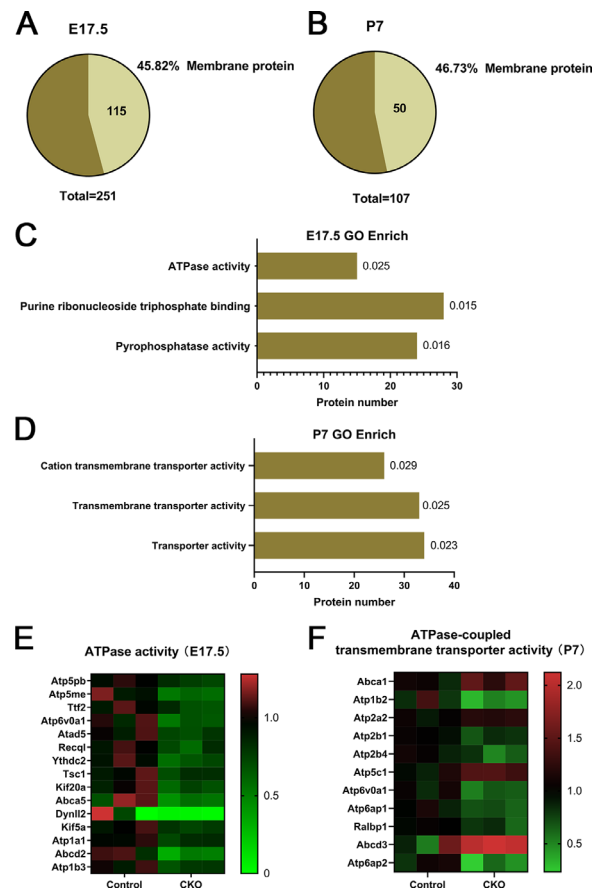


**FIGURE 5. Proteomic analysis of E17.5 and P7 mouse retinas.** (A, B) Pie charts showing the proportion of membrane proteins in E17.5 **A** and P7 **B** mice among the differential proteins based on proteomic analysis. (C, D) GO enrichment graphs showed the proportion of membrane proteins in E17.5 **C** and P7 **D** mice among the differential proteins. The numbers to the right of the bars are the ratio of the differential protein relative to the total protein in the pathway,  $P < 0.01$ . (E, F) Heatmap of the differential proteins involved in ATPase activity in E17.5 mice **E** and ATPase-coupled transmembrane transporter activity in P7 mice **F**. Proteins were categorized by ToppGene and colored by fold changes. All proteins were normalized by the average of control retinas. Details of the  $P$  values and fold changes are available in Supplementary Tables S1 and S2.

UPR pathway also increased in the CKO mice retina at P0.5 (Fig. 6B). Our TUNEL assay data also showed that apoptotic cells were increased in CKO mice retinas from E15.5 to P0.5 (Fig. 6C). This indicated that EMC3 deficiency caused the ERS response in retinal cells and eventually led to apoptosis.

### EMC3 Affects Retinal Neurogenesis

Because the loss of EMC3 could lead to serious retinal degeneration (see Fig. 2, Fig. 3), we sought to determine if it plays a role in retinal neurogenesis. First, we detected changes in the outer nuclear layer, which was the most seriously degenerated area. In P0.5 CKO mice retinas, the recoverin<sup>+</sup> photoreceptor cells changed from being spindle-shaped and regularly arranged at the apical regions of the retina to being rounded and unaligned. Some were even located in the middle of the retina, and the number of recoverin-positive cells increased by about 30% ( $P < 0.05$ ; Fig. 7A). Additionally, proteomic analysis showed that the expression of

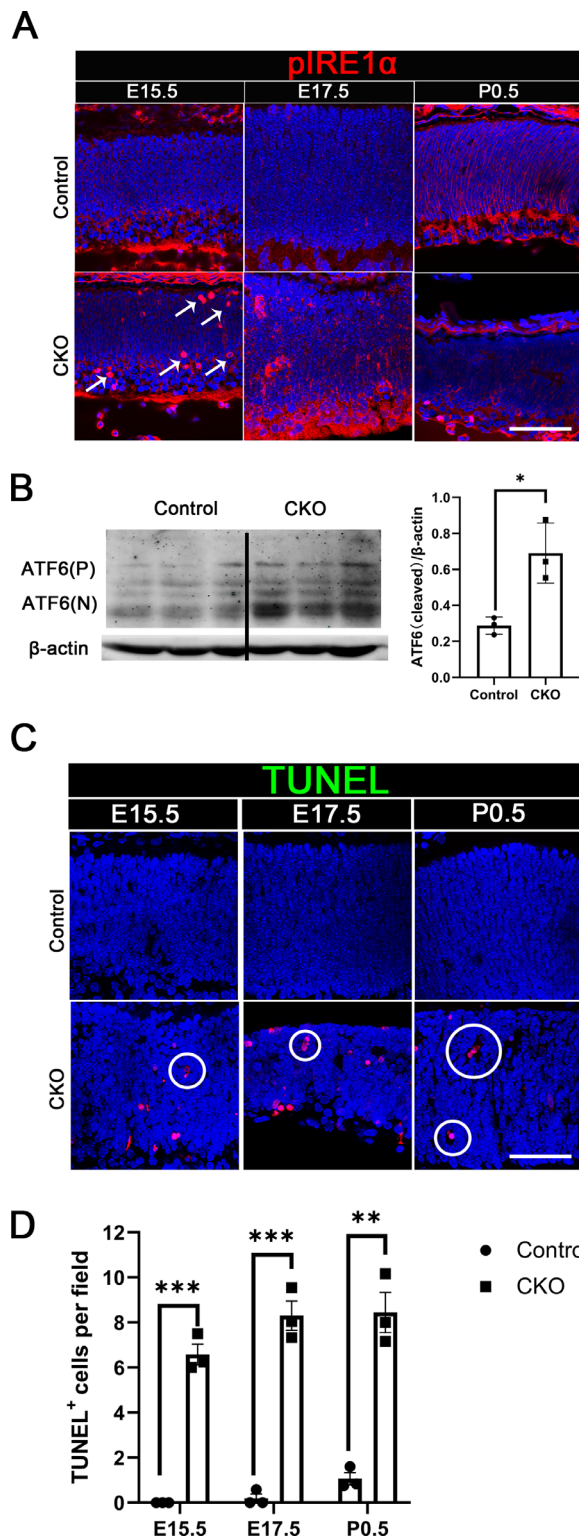


**FIGURE 6.** Deletion of EMC3 activates the ERS response and apoptosis. (A) E15.5, E17.5, and P0.5 retinal cryostat sections were immunostained with an antibody for pIRE1 $\alpha$  (red). White arrows indicate the cells with activated IRE1 $\alpha$ . (B) Western blot and quantitation were performed to detect ATF6 (50 kDa). (C) TUNEL assay (green) indicated apoptosis, which appeared in CKO mouse retinas beginning at E15.5. White circles show that apoptotic cells appeared in the center of the rosettes. Scale bars: 50  $\mu$ m.

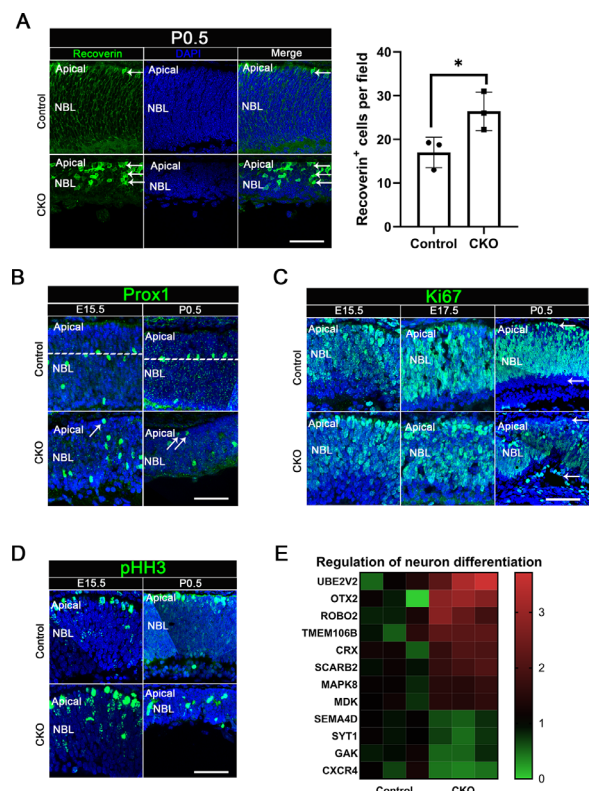


**FIGURE 7.** Loss of EMC3 affected the neurogenesis and positional changes of photoreceptor cells and horizontal cells. (A) Recoverin-marked (green) photoreceptors in P0.5 mice. Photoreceptors appeared in the retinal apical region in control mice. DAPI (blue) was used as a nuclear marker. The histogram on the right represents the number of cells per field. RPE, retinal pigment epithelium; NBL, neuroblastic layer; Scale bars: 50  $\mu$ m. (B) Immunofluorescence indicates that horizontal cells (Prox1 $^{+}$ , green) were dislocated in E15.5 and P0.5 CKO mice. Prox1 $^{+}$  cells are arranged close to the dotted line in the control mice. (C) Ki67-marked (green) cells (RPCs) in E15.5, E17.5, and P0.5 mice. Ki67 $^{+}$  cells disappeared in the apical region of the P0.5 CKO mouse retina. (D) Immunofluorescence indicates that cells in mitosis (pHH3 $^{+}$ , green) were dislocated in E15.5 and P0.5 CKO mice. (E) Heatmap of the differential proteins involved in the regulation of neural differentiation in E17.5 mouse retina.

Orthodenticle Homeobox 2 (OTX2) and cone-rod homeobox protein (CRX), both important proteins in the regulation of photoreceptor cell differentiation,<sup>41–43</sup> increased in CKO mice retinas (Fig. 7E). Horizontal cells are critical to the formation of the lamina.<sup>44</sup> Immunofluorescence showed that the location of Prox1 $^{+}$  horizontal cells was mislocated (Fig. 7B). Furthermore, the number of bipolar cells, Müller cells, amacrine cells, and ganglion cells were shown in P7 CKO mice retinas (Supplementary Figs. S6–S8), but the cell ratio in the retina did not change (Supplementary Fig. S9).

Early onset of apoptosis in the CKO mouse retina causes severe retinal degeneration in the later stage of retinal development,<sup>45</sup> making it difficult to distinguish the individual effects of neurogenesis. In addition, neural stem cells have different proliferative characteristics and roles in different developmental stages, which are also important for retinal lamination.<sup>30,46</sup> Therefore, we also studied the proliferative process of RPCs using Ki67.<sup>47</sup> Interestingly, Ki67 $^{+}$  cells in the apical region of the retina, which is the main location of mitotic RPCs,<sup>11</sup> decreased in CKO mice retinas at P0.5

(Fig. 7C). Next, staining of the mitotic marker phosphorylated histone H3 (pH 3)<sup>48</sup> showed that the distribution of mitotic progenitor cells was markedly scattered in the CKO mouse retina (Fig. 7D).

## DISCUSSION

Multiple studies have shown that EMC3 plays significant roles in rhodopsin synthesis and photoreceptor cell survival in *Drosophila*, zebrafish, and mice.<sup>19,25,26</sup> However, the roles of EMC3 in the retinal structure and neurogenesis during mammalian retinal development are unclear. The present study revealed several important findings regarding roles of EMC3 in retinal development. First, EMC3 was continuously expressed in various cells of the retina from embryo to adult mice. Second, the retina-specific knockout of the *Emc3* gene caused retinal rosette degeneration with mislocalization of some cell junction and polarity proteins in the early stages of mouse retinal development. Third, EMC3 may affect the stability of transmembrane proteins, especially ATPases. Furthermore, EMC3 is essential for the neurogenesis of photoreceptor cells and the distribution of retinal cells.

Our results show that the *Emc3* gene is expressed in the entire retinal layer throughout the development of mouse retina, including at P7. Thus, EMC3 is expressed both in RPCs and differentiated cells. These results are consistent with the highly conserved nature and ubiquity of EMC3 expression.<sup>12,13</sup> Our results are consistent with the single-cell sequencing study published in 2019.<sup>31</sup> However, reports on the mature retina have found that the EMC3 is mainly localized in the outer segment of photoreceptor cells.<sup>29</sup> The difference in findings may be due to the age of mice and the detection methods.

The retina is an extremely ordered structure.<sup>46</sup> We found that the absence of EMC3 during retinal development caused the formation of retinal rosettes, a typical pathological structure. This is the first time that structural lesions of tissues caused by EMC3 have been found. Over time during development, the retina became increasingly thinner, and most cells disappeared. However, although EMC3 can affect rhodopsin biosynthesis,<sup>26</sup> *Rbo* (rhodopsin gene) knockout in mice only affects photoreceptor cell density and does not cause retinal rosette degeneration.<sup>49</sup> These data suggest that EMC3 is essential for the correct structural development of the retina and that EMC3 deletion affects more than rhodopsin synthesis and photoreceptor cell survival.

The formation and maintenance of the retinal structure require the participation of cell junction molecules, such as  $\beta$ -catenin, N-cadherin, and ZO-1, and cell polarity molecules, such as Par6 / Par3 / PKC $\zeta$ . Our results showed that the knockout of *Emc3* in mouse retina resulted in the mislocalization of these cell junction and polarity molecules. However, studies based on Western blotting in CKO mice showed that the quantities of these proteins were close to those in control mice, supporting previous studies on the activity of EMC3 inserting enzymes.<sup>22</sup> These data indicate that the EMC3 affects retinal structural formation not by affecting the biosynthesis of these adhesion and polarity molecules, but by regulating the localization of these molecules.

Furthermore, proteomic analysis of CKO mice retinas revealed that transmembrane proteins were the main type of downregulated proteins, and gene ontology analysis enriched out ATPase activity-related proteins.

ATPase activity-related proteins are mainly membrane pump proteins responsible for ion transport. These proteins play important roles in regulating cell polarity,<sup>50-52</sup> motility, metabolism, growth, and apoptosis.<sup>38,53-56</sup> For example, *Atp6v0c* and *Atp6v0a3* mutations and *Atp6ap2* deletion lead to retinal degeneration.<sup>35</sup> ATP6AP2 interacts with Par3 and contributes to laminar formation during retinal development.<sup>51</sup> Interestingly, our results also revealed that retinal *Emc3* knockout results in the same pathological pattern as *Atp6ap2* deletion, including a change in Par3 localization without changes in protein expression. We speculated that EMC3 regulates the stability of these ATPase proteins, leading to the disordering of the retinal structure.

EMC3 plays an important role in regulating protein processing and folding, whereas protein misfolding tends to cause UPR and ERS. We found that the expression levels of several key ERS pathway proteins were elevated, and the percentage of apoptotic cells also increased. This indicates that EMC3 deficiency can activate the ERS response of retinal cells and eventually lead to apoptosis.

It is not clear if EMC3 regulates neurogenesis in the retina. Here, we found that loss of retinal EMC3 led to increased differentiation of photoreceptor cells. Proteomic data also showed increased levels of OTX2 and CRX levels in CKO mice retinas. *Otx2* is a key regulatory gene for cell fate determination of retinal photoreceptor cells, and it transactivates the *Crx* gene, which is necessary for the terminal differentiation and maintenance of photoreceptor cells.<sup>41-43</sup> This suggests that deletion of retinal EMC3 can increase the neurogenesis of photoreceptors and affect the localization of several retinal cells. However, our H&E results also showed that the photoreceptor cell layer was reduced in the CKO mice. This is consistent with a previous study revealing that EMC3 is essential for the survival of photoreceptors.<sup>26</sup> This reflects a balance between the complex roles of EMC3 in cell differentiation and apoptosis, and this balance is different for different cells. Our data showed that EMC3 loss also affects the localization of several retinal cells, suggesting a wide range of functions in the retina.

In conclusion, our findings revealed that EMC3 is essential in the development of mouse retina, and it not only participates in retinal neurogenesis, but also regulates retinal structure. EMC3 regulates retinal structure by maintaining the polarity of RPCs and regulating ATPase-related proteins. In addition, EMC3 can affect the neurogenesis of photoreceptors and the distribution of retinal cells. This study not only fills a gap in our understanding of the development of the mammalian retina but can also be used as a reference for the study of retinoblastoma pathology.

## Acknowledgments

The authors thank Shanghai Applied Protein Technology Co., LTD, for help with the proteomic analysis.

Supported by Zhejiang Provincial Natural Science Foundation of China under Grant No. LQ18H120009.

**Author Contributions:** X.C. and J.A. generated and bred the conditional knockout of *Emc3*. J.A., X.L., and X.Z. designed experiments. X.C. and Y.C. performed morphological and RNAscope in situ hybridization. J.A. and J.L. performed OCT and ERG experiments. X.C. and J.A. performed immunofluorescence, TUNEL, Western blot, and proteomics experiments. X.C.,

J.W., and Y.D. analyzed the data. X.C., J.A., Y.D., X.L., and X.Z. wrote the manuscript.

Disclosure: **X. Cao**, None; **J. An**, None; **Y. Cao**, None; **J. Lv**, None; **J. Wang**, None; **Y. Ding**, None; **X. Lin**, None; **X. Zhou**, None

## References

- Hinds JW, Hinds PL. Early ganglion cell differentiation in the mouse retina: an electron microscopic analysis utilizing serial sections. *Dev Biol.* 1974;37:381–416.
- Young RW. Cell differentiation in the retina of the mouse. *Anat Rec.* 1985;212:199–205.
- Turner DL, Cepko CL. A common progenitor for neurons and glia persists in rat retina late in development. *Nature.* 1987;328:131–136.
- Cepko CL, Austin CP, Yang X-J, Alexiades M, Ezzeddine D. Cell fate determination in the retina. *Proc Natl Acad Sci USA.* 1996;93:589–595.
- Randlett O, Norden C, Harris WA. The vertebrate retina: a model for neuronal polarization in vivo. *Dev Neurobiol.* 2011;71:567–583.
- Fu X, Sun H, Klein WH, Mu X. Beta-catenin is essential for lamination but not neurogenesis in mouse retinal development. *Dev Biol.* 2006;299:424–437.
- Erdmann B, Kirsch FP, Rathjen FG, More MI. N-cadherin is essential for retinal lamination in the zebrafish. *Dev Dyn.* 2003;226:570–577.
- Masai I, Lele Z, Yamaguchi M, et al. N-cadherin mediates retinal lamination, maintenance of forebrain compartments and patterning of retinal neurites. *Development.* 2003;130:2479–2494.
- Miyamoto Y, Sakane F, Hashimoto K. N-cadherin-based adherens junction regulates the maintenance, proliferation, and differentiation of neural progenitor cells during development. *Cell Adb Migr.* 2015;9:183–192.
- Wei X, Cheng Y, Luo Y, Shi X, Nelson S, Hyde DR. The zebrafish *Pard3* ortholog is required for separation of the eye fields and retinal lamination. *Dev Biol.* 2004;269:286–301.
- Koike C, Nishida A, Akimoto K, et al. Function of atypical protein kinase C lambda in differentiating photoreceptors is required for proper lamination of mouse retina. *J Neurosci.* 2005;25:10290–10298.
- Jonikas MC, Collins SR, Denic V, et al. Comprehensive characterization of genes required for protein folding in the endoplasmic reticulum. *Science.* 2009;323:1693.
- Wideman JG. The ubiquitous and ancient ER membrane protein complex (EMC): tether or not? *F1000Res.* 2015;4:624.
- Christianson JC, Olzmann JA, Shaler TA, et al. Defining human ERAD networks through an integrative mapping strategy. *Nat Cell Biol.* 2011;14:93–105.
- Li Y, Zhao Y, Hu J, et al. A novel ER-localized transmembrane protein, EMC6, interacts with RAB5A and regulates cell autophagy. *Autophagy.* 2013;9:150–163.
- Richard M, Boulton T, Robert VJ, Richmond JE, Bessereau JL. Biosynthesis of ionotropic acetylcholine receptors requires the evolutionarily conserved ER membrane complex. *Proc Natl Acad Sci USA.* 2013;110:E1055–E1063.
- Lahiri S, Chao JT, Tavassoli S, et al. A conserved endoplasmic reticulum membrane protein complex (EMC) facilitates phospholipid transfer from the ER to mitochondria. *PLoS Bio.* 2014;12:e1001969.
- Ma H, Dang Y, Wu Y, et al. A CRISPR-based screen identifies genes essential for west-nile-virus-induced cell death. *Cell Rep.* 2015;12:673–683.
- Satoh T, Ohba A, Liu Z, Inagaki T, Satoh AK. dPob/EMC is essential for biosynthesis of rhodopsin and other multi-pass membrane proteins in Drosophila photoreceptors. *Elife.* 2015;4:e06306.
- Shen X, Kan S, Hu J, et al. EMC6/TMEM93 suppresses glioblastoma proliferation by modulating autophagy. *Cell Death Dis.* 2016;7:e2043.
- Tang X, Snowball JM, Xu Y, et al. EMC3 coordinates surfactant protein and lipid homeostasis required for respiration. *J Clin Invest.* 2017;127:4314–4325.
- Chitwood PJ, Juszkievicz S, Guna A, Shao S, Hegde RS. EMC is required to initiate accurate membrane protein topogenesis. *Cell.* 2018;175:1507–1519.e1516.
- Volkmar N, Thezenas M-L, Louie SM, et al. The ER membrane protein complex promotes biogenesis of sterol-related enzymes maintaining cholesterol homeostasis. *J Cell Sci.* 2019;132:jcs223453.
- Brockerhoff SE, Hurley JB, Niemi GA, Dowling JE. A new form of inherited red-blindness identified in zebrafish. *J Neurosci.* 1997;17:4236–4242.
- Taylor MR, Kikkawa S, Diez-Juan A, et al. The zebrafish *pob* gene encodes a novel protein required for survival of red cone photoreceptor cells. *Genetics.* 2005;170:263–273.
- Xiong L, Zhang L, Yang Y, et al. ER complex proteins are required for rhodopsin biosynthesis and photoreceptor survival in Drosophila and mice. *Cell Death Differ.* 2019;27(2):646–661.
- Furuta Y, Lagutin O, Hogan BL, Oliver GC. Retina- and ventral forebrain-specific Cre recombinase activity in transgenic mice. *Genesis.* 2000;26:130–132.
- Wang F, Flanagan J, Su N, et al. RNAscope: a novel in situ RNA analysis platform for formalin-fixed, paraffin-embedded tissues. *J Mol Diagn.* 2012;14:22–29.
- Ma J, Chen T, Wu S, et al. iProX: an integrated proteome resource. *Nucleic Acids Res.* 2019;47:D1211–D1217.
- Cepko CL, Austin CP, Yang X, Alexiades M, Ezzeddine D. Cell fate determination in the vertebrate retina. *Proc Natl Acad Sci USA.* 1996;93:589.
- Peng YR, Shekhar K, Yan W, et al. Molecular classification and comparative taxonomics of foveal and peripheral cells in primate retina. *Cell.* 2019;176:1222–1237.e1222.
- Eagle RC. The pathology of ocular cancer. *Eye (Lond).* 2013;27:128–136.
- Andersen SR. Differentiation features in some retinal tumors and in dysplastic retinal conditions. *Am. J. Ophthalmol.* 1971;71:231–241.
- Lahav M, Albert DM, Craft JL. Light and electron microscopic study of dysplastic rosette-like structures occurring in the disorganized mature retina. *Albrecht von Graefes Arch Klin Exp Ophthalmol.* 1975;195:57–68.
- Nuckels RJ, Ng A, Darland T, Gross JM. The vacuolar-ATPase complex regulates retinoblast proliferation and survival, photoreceptor morphogenesis, and pigmentation in the zebrafish eye. *Invest Ophthalmol Vis Sci.* 2009;50:893–905.
- Satoh T, Inagaki T, Liu Z, Watanabe R, Satoh AK. GPI biosynthesis is essential for rhodopsin sorting at the trans-Golgi network in Drosophila photoreceptors. *Development.* 2013;140:385–394.
- Jaiswal M, Haelterman NA, Sandoval H, et al. Impaired mitochondrial energy production causes light-induced photoreceptor degeneration independent of oxidative stress. *PLoS Biol.* 2015;13:e1002197.
- Colacurcio DJ, Nixon RA. Disorders of lysosomal acidification - the emerging role of v-ATPase in aging and neurodegenerative disease. *Ageing Res Rev.* 2016;32:75–88.
- Harding HP, Zhang Y, Ron D. Protein translation and folding are coupled by an endoplasmic-reticulum-resident kinase. *Nature.* 1999;397:271–274.



40. Hampton RY. ER stress response: getting the UPR hand on misfolded proteins. *Curr Biol.* 2000;10:R518–521.
41. Nishida A, Furukawa A, Koike C, et al. Otx2 homeobox gene controls retinal photoreceptor cell fate and pineal gland development. *Nat Neurosci.* 2003;6:1255–1263.
42. Koike C, Nishida A, Ueno S, et al. Functional roles of Otx2 transcription factor in postnatal mouse retinal development. *Mol Cell Biol.* 2007;27:8318–8329.
43. Ghinia Tegla MG, Buenaventura DF, Kim DY, Takurdin C, Gonzalez KC, Emerson MM. OTX2 represses sister cell fate choices in the developing retina to promote photoreceptor specification. *Elife.* 2020;9:e54279.
44. Dyer MA, Livesey FJ, Cepko CL, Oliver G. Prox1 function controls progenitor cell proliferation and horizontal cell genesis in the mammalian retina. *Nat Genet.* 2003;34:53–58.
45. Bassett EA, Wallace VA. Cell fate determination in the vertebrate retina. *Trends Neurosci.* 2012;35:565–573.
46. Nguyen-Ba-Charvet KT, Chédotal A. Development of retinal layers. *C R Biol.* 2014;337:153–159.
47. Gerdes J, Lemke H, Baisch H, Wacker HH, Schwab U, Stein H. Cell cycle analysis of a cell proliferation-associated human nuclear antigen defined by the monoclonal antibody Ki-67. *J Immunol.* 1984;133:1710–1715.
48. Prigent C, Dimitrov S. Phosphorylation of serine 10 in histone H3, what for? *J Cell Sci.* 2003;116:3677–3685.
49. Wang R, Jiang C, Ma J, Young MJ. Monitoring morphological changes in the retina of rhodopsin<sup>-/-</sup> mice with spectral domain optical coherence tomography. *Invest Ophthalmol Vis Sci.* 2012;53:3967–3972.
50. Hermle T, Saltukoglu D, Grunewald J, Walz G, Simons M. Regulation of Frizzled-dependent planar polarity signaling by a V-ATPase subunit. *Curr Biol.* 2010;20:1269–1276.
51. Kanda A, Noda K, Yuki K, et al. Atp6ap2/(pro)renin receptor interacts with Par3 as a cell polarity determinant required for laminar formation during retinal development in mice. *J Neurosci.* 2013;33:19341–19351.
52. Schafer ST, Han J, Pena M, von Bohlen Und Halbach O, Peters J, Gage FH. The Wnt adaptor protein ATP6AP2 regulates multiple stages of adult hippocampal neurogenesis. *J Neurosci.* 2015;35:4983–4998.
53. Zacchi LF, Wu HC, Bell SL, et al. The BiP molecular chaperone plays multiple roles during the biogenesis of torsinA, an AAA+ ATPase associated with the neurological disease early-onset torsion dystonia. *J Biol Chem.* 2014;289:12727–12747.
54. Cotter K, Stransky L, McGuire C, Forgac M. Recent insights into the structure, regulation, and function of the V-ATPases. *Trends Biochem Sci.* 2015;40:611–622.
55. Pamarthy S, Mao L, Katara GK, et al. The V-ATPase  $\alpha 2$  isoform controls mammary gland development through Notch and TGF-beta signaling. *Cell Death Dis.* 2016;7:e2443.
56. Pamarthy S, Kulshrestha A, Katara GK, Beaman KD. The curious case of vacuolar ATPase: regulation of signaling pathways. *Mol Cancer.* 2018;17:41.